Journal of Cellular Biochemistry Supplement 36:19–31 (2001)

Nuclear Changes in Necrotic HL-60 Cells

Roberta Bortul,[1] Marina Zweyer,[1] Anna Maria Billi,[2] Giovanna Tabellini,[1] Robert L. Ochs,[3] Renato Bareggi,[1] Lucio Cocco,[2] and Alberto M. Martelli[1,2]*

[1]Dipartimento di Morfologia Umana Normale, Università di Trieste, 34138 Trieste, Italy
[2]Dipartimento di Scienze Anatomiche Umane e Fisiopatologia dell'Apparato Locomotore, Facoltà di Farmacia, Università di Bologna, 40126 Bologna, Italy
[3]Precision Therapeutics, Pittsburgh, PA 15213, Pennsylvania

Abstract Cell death in eukaryotes can occur by either apoptosis or necrosis. Apoptosis is characterized by well-defined nuclear changes which are thought to be the consequence of both proteolysis and DNA fragmentation. On the other hand, the nuclear modifications that occur during necrosis are largely less known. Here, we have investigated whether or not nuclear modifications occur during ethanol-induced necrotic cell death of HL-60 cells. By means of immunofluorescence staining, we demonstrate that the patterns given by antibodies directed against some nuclear proteins (lamin B1, NuMA, topoisomerase IIα, SC-35, B23/nucleophosmin) changed in necrotic cells. The changes in the spatial distribution of NuMA strongly resembled those described to occur during apoptosis. On the contrary, the fluorescent pattern characteristic for other nuclear proteins (C23/nucleolin, UBF, fibrillarin, RNA polymerase I) did not change during necrosis. By immunoblotting analysis, we observed that some nuclear proteins (SAF-A, SATB1, NuMA) were cleaved during necrosis, and in the case of SATB1, the apoptotic signature fragment of 70 kDa was also present to the same extent in necrotic samples. Caspase inhibitors did not prevent proteolytic cleavage of the aforementioned polypeptides during necrosis, while they were effective if apoptosis was induced. In contrast, lamin B1 and topoisomerase IIα were uncleaved in necrotic cells, whereas they were proteolyzed during apoptosis. Transmission electron microscopy analysis revealed that slight morphological changes were present in the nuclear matrix fraction prepared from necrotic cells. However, these modifications (mainly consisting of a rarefaction of the inner fibrogranular network) were not as striking as those we have previously described in apoptotic HL-60 cells. Taken together, our results indicate that during necrosis marked biochemical and morphological changes do occur at the nuclear level. These alterations are quite distinct from those known to take place during apoptosis. Our results identify additional biochemical and morphological criteria that could be used to discriminate between the two types of cell death. J. Cell. Biochem. Suppl. 36:19–31, 2001.

Key words: necrosis; apoptosis; proteolysis; caspases; nuclear proteins; nuclear matrix

Two morphologically distinct pathophysiological types of cell death which occur in eukaryotes are apoptosis and necrosis. While apoptosis is genetically controlled and is defined by nuclear and cytoplasmic shrinkage, membrane blebbing, chromatin margination, and DNA fragmentation, necrosis is characterized by nuclear pyknosis, cytoplasmic swelling, and a progressive loss of membrane integrity [Wyllie et al., 1980; Bellamy et al., 1995]. During apoptosis the cell is broken down in multiple spherical bodies that retain membrane integrity and are phagocytosed by neighboring cells without eliciting significant inflammatory damage [Bellamy et al., 1995]. In necrosis, cellular fragmentation takes place with a subsequent release of lysosomal content in the extracellular space and the occurrence of inflammation [Wyllie et al., 1980].

Recent findings have highlighted the fact that the differences between necrosis and apoptosis

Grant sponsor: Italian "MURST Cofinanziamento 1999" to A. M. Martelli and L. Cocco; Grant sponsor: Associazione Italiana per la Ricerca sul Cancro (AIRC) to L. Cocco; Grant sponsor: Funds For Selected Research Topics of Bologna University and the Italian CNR Finalized Project "Biotechnology" to L. Cocco; Grant sponsor: Italian Ministry for Health "Ricerca Finalizzata" to A.M. Martelli.

*Correspondence to: Dr. Alberto M. Martelli, Dipartimento di Morfologia Umana Normale, Università di Trieste, via Manzoni 16,34138 Trieste, Italy. E-mail: martelli@univ.trieste.it

Received 3 October 2000; Accepted 30 November 2000

This article published online in Wiley InterScience, March 13, 2001.

might be less numerous than initially believed. Indeed, some of the biochemical changes which take place during apoptosis have been reported to occur also during necrosis. For example, the inner mitochondrial membrane may become permeable to ions and small molecules during both necrosis and apoptosis. Moreover, activation of cysteine proteases and cleavage of poly(ADP-ribose) polymerase has been documented to occur during both modes of cell death [Shah et al., 1996; Dynlacht et al., 1999].

A central biochemical mechanism that leads to apoptotic cell death is the activation of a family of cysteinyl-aspartate-specific proteases referred to as caspases [Patel et al., 1996; Thornberry and Lazebnik, 1998; Utz and Anderson, 2000]. Most of the proteins cleaved by caspases have important functions in the cell, so that their cleavage during early stages of apoptosis may be expected to silence basic cellular processes and to lead to disintegration of cellular architecture. However, evidence suggests that protease activation is also important for cell necrosis and in some cases caspase activation has been reported to occur during this type of cell death [e.g. Shimizu et al., 1996; Faraco et al., 1999].

A distinctive feature of apoptotic cell death are the marked changes occurring in the nucleus, which most likely reflect proteolysis of several polypeptides and fragmentation of DNA [Earnshaw, 1995; Martelli et al., 1997]. Indeed, several nuclear protein are targets of activated proteases and include: topoisomerase I, topoisomerase IIα, lamins, lamin B receptor, NuMA, SAF-A, UBF, SATB1, heterogeneous ribonucleoproteins C1 and C2, U1-70 kDa [Earnshaw, 1995; Casiano et al., 1996; Waterhouse et al., 1996; Weaver et al., 1996; Goehring et al., 1997; Duband-Goulet et al., 1998; Buendia et al., 1999; Gotzmann et al., 2000; see Martelli et al., 1997 for a comprehensive review on the issue]. Moreover, recent findings indicate that the apoptotic process is also characterized by a caspase-mediated cleavage of nucleic acids through the activation of nucleolytic activities [Degen et al., 2000]. During apoptosis, modifications have been described to occur in the nuclear matrix, i.e. the proteinaceous structure which is thought to be responsible for maintaining the functional and topological organization of the interphase nucleus [Berezney et al., 1995; Martelli et al., 1996, 1999a, 1999b]. In particular, a disassembly of the nuclear matrix is thought to be a critical step which leads to nuclear collapse [Weaver et al., 1996; Martelli et al., 1997; Gerner et al., 1998]. On the other hand, the changes that take place in the necrotic nucleus have scarcely been investigated, even though proteolysis of some key nuclear proteins has been reported to also occur during necrotic cell death [Casiano et al., 1998]. In particular, Dynlacht et al. [1999] recently suggested that degradation of nuclear matrix is a common element during both apoptosis and necrosis induced by irradiation of HL-60 cells. However, they came to such a conclusion exclusively by observing that lamin B was proteolytically cleaved during the necrotic process. Therefore, we decided to perform a comprehensive investigation of the nuclear structure during ethanol-induced necrosis of HL-60 cells. Our results show that most of the changes in the distribution of several key nuclear components which occur during necrosis are clearly distinct from those described during apoptosis and the same is true for the proteolysis of select nuclear polypeptides. In addition, we show that slight modifications of the nuclear matrix also occur during necrosis as demonstrated by ultrastructural analysis, albeit the changes are not as striking as during apoptosis.

MATERIALS AND METHODS

Source of Antibodies and Caspase Inhibitors

The following antibodies were employed in this study: monoclonal antibody to topoisomerase IIα (clone Ki-S1, Roche Molecular Biochemicals, Milan, Italy); monoclonal antibody to NuMA N-terminal head domain (Transduction Laboratories, Lexington, KY); monoclonal antibody to lamin B1 (clone 101-B7, Calbiochem, La Jolla, CA); monoclonal antibodies to splicing factor SC-35 or β-tubulin (Sigma Chemical Company, St. Louis, MO); polyclonal antibody to protein SATB1 was a kind gift by Dr. Terumi Kohwi-Shigematsu, University of California, Berkeley, CA; polyclonal antibody to SAF-A was a generous gift by Dr. Frank Fackelmayer, University of Konstanz, Germany; monoclonal or polyclonal antibodies to nucleolar proteins (C23/nucleolin; B23/nucleophosmin; RNA polymerase I; UBF; fibrillarin) were as recently reported [Martelli et al., 2000]. The following cell-permeable irreversible caspase inhibitors were from Calbiochem: Ac-DEVD-CMK (an inhibitor of caspase-3); VEID-CHO (an inhibitor

of caspase-6); Z-IETD-FMK (an inhibitor of caspase-8); Z-LEHD-FMK (an inhibitor of caspase-9).

Cell Culture and Induction of Apoptosis or Necrosis

HL-60 human promyelocytic leukemia cells were cultured in RPMI-1640 medium supplemented with 10% fetal bovine serum. For induction of apoptosis, cells were exposed for 5 h to 68 μM etoposide (Sigma). Flow cytometric analysis revealed that this treatment caused about 85–90% of cells to undergo apoptosis, whereas in control samples $< 1\%$ of cells were apoptotic [data not shown and Martelli et al., 1999a]. For induction of necrosis, cells were exposed to 10% ethanol for 5 h [Casiano et al., 1998]. In the experiments performed in the presence of caspase inhibitors, the chemicals were added 30 min prior to adding etoposide or ethanol. The final concentration of the inhibitors was 100 μM, from a 25 mM stock in dimethylsulfoxide.

Transmission Electron Microscopy (TEM) Analysis

Cells or nuclear matrices were fixed with 2.5% glutaraldehyde in 0.1 M phosphate buffer for 35 min, dehydrated in increasing concentrations of acetone, embedded in Araldite, thin sectioned, and observed with a Jeol 100S electron microscope.

Immunofluorescence Staining

Cells were plated onto 0.1% poly-L-lysine-coated glass slides and adhesion was allowed to proceed for 30 min at 37°C. Samples were fixed in freshly-prepared 4% paraformaldehyde in PBS for 30 min at room temperature. After several washes with PBS, nonspecific binding of antibodies was blocked by a 30 min incubation at 37°C with blocking buffer, i.e. PBS containing 5% normal goat serum (NGS) and 4% bovine serum albumin (BSA, Sigma fraction V). Slides were then incubated for 3 h at 37°C with the primary antibodies diluted in blocking buffer. They were subsequently washed three times in PBS and reacted for 1 h at 37°C with the appropriate fluorescein isothiocyanate (FITC)-conjugated secondary antibodies (from Sigma), diluted 1:100 in blocking buffer. Samples were then stained for DNA with 0.1 μg/ml 4′-6-diamidino-2-phenylindole (DAPI) in PBS, 0.05% Tween 20. Slides were observed and photographed using a Zeiss Axiophot epifluorescence microscope.

Polyacrylamide Gel Electrophoresis and Immunoblotting of Cell Lysates

Cells were sedimented at 1,000*g* for 10 min and washed twice in phosphate buffered saline, pH 7.4 (PBS) containing the COMPLETE Protease Inhibitor Cocktail (Roche Molecular Biochemicals), according to the manufacturer's instructions. Cells were then resuspended at $\sim 10^7$/ml in boiling lysis buffer containing 62.5 mM Tris-HCl, pH 6.8, 2% sodium dodecylsulfate (SDS), 10% glycerol, 5% 2-mercaptoethanol, and the protease inhibitor cocktail. Lysates were briefly sonicated to shear DNA and reduce viscosity, boiled for 5 min to solubilize protein, and stored at -80°C until required. Cell harvesting and lysate preparation were conducted in the presence of the protease inhibitor cocktail as a precaution to prevent further proteolysis. Total protein from $\sim 5 \times 10^6$ cells was separated by SDS-polyacrylamide gel electrophoresis (SDS-PAGE) and electrophoretically transferred to nitrocellulose sheets using a semi-dry blotting apparatus (Hoefer/Pharmacia Biotech, Uppsala, Sweden). Sheets were saturated for 60 min at 37°C in blocking buffer, then incubated overnight at 4°C in blocking buffer containing the primary antibodies. After four washes in PBS containing 0.1% Tween 20, they were incubated for 30 min at room temperature with peroxidase-conjugated secondary antibodies (from Sigma), diluted 1:5,000 in PBS-Tween 20, and washed as above. Bands were visualized by the enhanced chemiluminescence method using Lumi-Light^{Plus} (Roche Molecular Biochemicals).

Preparation of Nuclear Matrix from HL-60 Cells

Cells were washed once in PBS (without Ca^{2+} and Mg^{2+}) and resuspended to 1.5×10^7/ml in 10 mM Tris-HCl, pH 7.4, 2 mM $MgCl_2$, 0.5 mM phenylmethylsulfonyl fluoride (PMSF), 1 μg/ml each of aprotinin and leupeptin (TM-2 buffer, temperature = 10°C). After 5 min at 0°C, Triton X-100 was added to 0.5% (w/v) and cells were sheared by one passage through a 22 gauge needle fitted to a 30 ml plastic syringe. Nuclei were sedimented at 400*g* for 6 min, washed once in TM-2 buffer and resuspended to 2 mg DNA/ml in 10 mM Tris-HCl, pH 7.4, 0.25 M sucrose, 5 mM $MgCl_2$ plus protease inhibitors as above

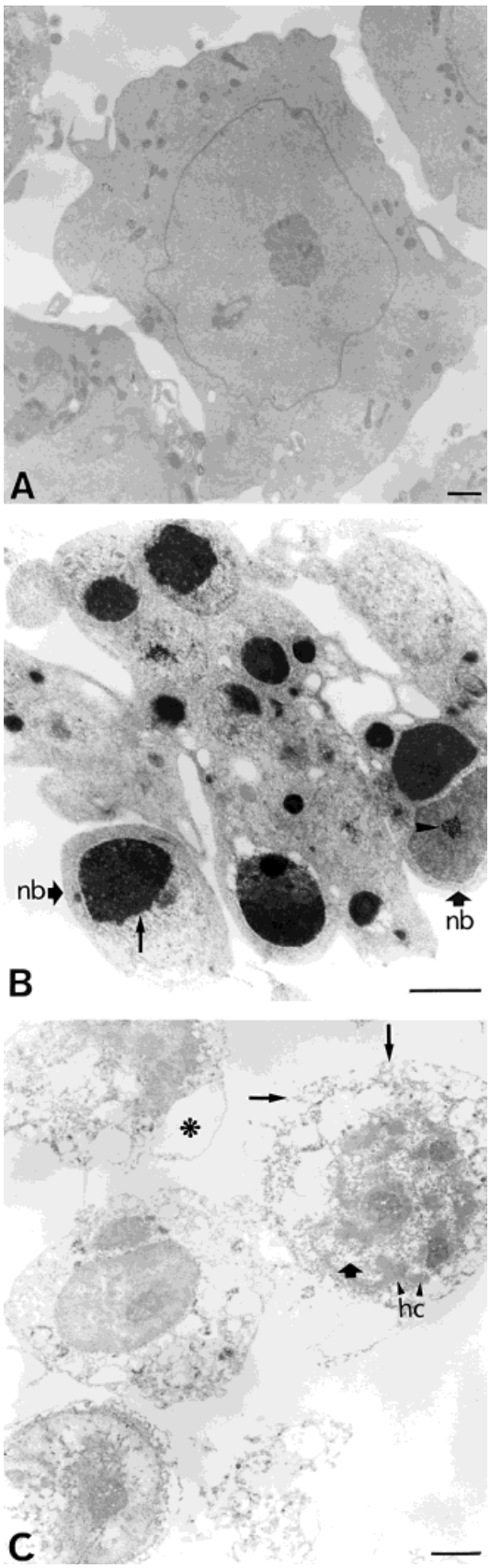

(STM-5 buffer). They were incubated for 45 min at 0°C in STM-5 buffer containing 2 mM sodium tetrathionate (NaTT). Nuclei were then digested for 60 min at 0°C with 50 U DNase I/mg DNA (from Sigma). An equal volume of 4 M NaCl in 10 mM Tris-HCl, pH 7.4, 0.2 mM $MgCl_2$, 1 mM PMSF (LM buffer) was then added, followed by 8 volumes of 2 M NaCl in LM buffer. Structures were sedimented at 1,500*g* for 10 min, washed once in LM buffer, and employed as the nuclear matrix fraction.

Protein Recovery

Assays Were Performed as Described by Bradford [1976].

Two-Dimensional Gel Electrophoresis

Nuclear matrix protein (from 5×10^7 cells) was resuspended in 400 μl of lysis buffer [O'Farrell, 1975] and incubated for 3 h at room temperature. Insoluble material was removed by centrifugation at 10,000*g* for 5 min and the supernatant was layered on the first dimension gel. Non-equilibrium pH gradient gel electrophoresis (NEPHGE) was carried out as reported by O'Farrell et al. [1977] in 9.2 M urea, 2% Nonidet P-40, 4% polyacrylamide, 2% ampholytes (Bio-Lyte pH 3-10, Bio-Rad Laboratories, Hercules, CA). First dimension gels (10 cm-long with a diameter of 3 mm) were run for 16 h at 300 V (constant). Second dimension gels were 8% SDS-PAGE. Gels were stained with Coomassie Blue R-250. The pH gradient was calibrated using carbamylated glyceraldehyde-3-phosphate dehydrogenase standards (Pharmacia Biotech). Gels representative of three separate preparations are shown.

RESULTS

TEM Analysis of HL-60 Cells

As presented in Figure 1A, the ultrastructural morphology of control HL-60 cells was typical. Nuclei were indented, with a prevalence of euchromatin and one or more evident

Fig. 1. TEM analysis of control, apoptotic, and necrotic HL-60 cells. (**A):** control (untreated) cell. (**B):** apoptotic (etoposide-incubated) cell; nb: nuclear body; arrow points to chromatin marginations while arrowhead indicates a nucleolar segregation. (**C):** ethanol-exposed cell; hc: heterochromatin; asterisk indicates a large cytoplasmic vacuole; arrowhead indicates a transparent area, which is often seen in necrotic nuclei; arrows points to the damaged plasma membrane. Scale bar: 1 μm.

nucleoli. In cells exposed for 5 h to etoposide, the distinctive apoptotic nuclear bodies were observed. The plasma membrane was well conserved even at this late stage (Fig. 1B). In approximately 90% of ethanol-treated cells we observed a heavily damaged and swollen cytoplasm containing numerous vacuoles of different size (Fig. 1C). The plasma membrane showed several breaks. The nucleus was still surrounded by a well preserved envelope. Numerous small and regular clumps of heterochromatin were scattered in the nuclear interior and juxtaposed to the nuclear envelope (Fig. 1C). It is important to emphasize that in necrotic samples we did not ever detect the ultrastructural nuclear changes which are characteristic of apoptotic cell death, such as chromatin margination, nucleolar segregation, and the appearance of nuclear inclusions referred to as HERDS [Earnshaw, 1995; Zweyer et al., 1995, 1997; Biggiogera et al., 1999; Martelli et al., 2000].

Immunofluorescence Staining of Nuclear Antigens in Necrotic HL-60 Cells

We next investigated by fluorescent immunostaining whether or not changes in the distribution of nuclear proteins occurred during necrosis. Antibody to lamin B1 decorated the nuclear periphery in normal HL-60 cells, delineating a ring (Fig. 2). In necrotic samples, besides the nuclear periphery, the antibody also stained the nuclear interior (Fig. 2). The monoclonal antibody recognizing topoisomerase IIα revealed a sort of fibrogranular network in normal cells, and spared nucleoli that were outlined by DAPI staining (Fig. 2). In necrotic HL-60 cells, the antibody characteristically stained extremely bright and large (diameter: 2–3.5 μm) clumps as well as smaller dots (Fig. 2). Interestingly, DAPI counterstaining revealed that both the smaller dots and the large clumps were located within the nucleoli. In control cells, antibody to NuMA gave a staining pattern distribution similar to topoisomerase IIα (Fig. 2). In necrotic nuclei we detected numerous brilliant spots of different size, which localized both to the center and the periphery (Fig. 2). Monoclonal antibody to the essential splicing component SC-35 immunostained numerous (20–25 for each nucleus) spots, of different size, located both in the center and at the periphery of the control nuclei (Fig. 2). In necrotic samples, the spots were somewhat smaller and mostly concentrated at the nuclear periphery (Fig. 2).

We next investigated a group of proteins that were localized to the nucleolus of control cells. The fluorescent immunostaining due to antibodies recognizing the majority of these proteins (fibrillarin, UBF, C23/nucleolin, RNA polymerase I) did not change in necrotic cells (Fig. 2). In necrotic samples we did not observe any positive immunostaining of nucleoli when we employed a monoclonal antibody to protein B23/nucleophosmin which, on the other hand, produced a very bright reaction when used in normal samples (Fig. 2). However, some faint immunoreactivity was seen at the nuclear periphery of ethanol-treated cells. In Table I we report, for each of the antigens studied, the percentage of necrotic cells in which we detected the immunofluorescent pattern illustrated in the pictures. It is evident that the pattern we have chosen as "representative" was seen in the majority of necrotic cells.

Immunoblotting Analysis of Nuclear Proteins in HL-60 Cell Lysates and Effect of Caspase Inhibitors

In preliminary experiments, we examined the polypeptide composition of control, apoptotic, and necrotic cells by performing SDS-PAGE of whole cell extracts. As presented in Figure 3, Coomassie Blue staining of gels revealed no major differences between control and apoptotic cells. This was true also for extracts from necrotic cells apart from the presence of a very prominent band at 70 kDa. Overall, we feel that this observation may suggest that protein cleavage possibly observed in necrotic cells was unlikely to be due to massive release of compartmentalized proteases during cell lysis, in agreement with others [Casiano et al., 1998].

To determine whether or not also necrosis is associated with cleavage of key nuclear proteins, we examined 8 polypeptides by immunoblotting analysis of HL-60 whole cell lysates prepared from control (untreated), etoposide-treated (apoptotic), and ethanol-treated (necrotic) cells.

In apoptotic cells, lamin B1 was cleaved and we detected a 28 kDa fragment. Such a fragment was not present in necrotic cells, in which lamin B1 was largely uncleaved, even though we saw a very faint band at approximately 50 kDa (Fig. 4). Topoisomerase IIα was also cleaved during apoptosis with a predomi-

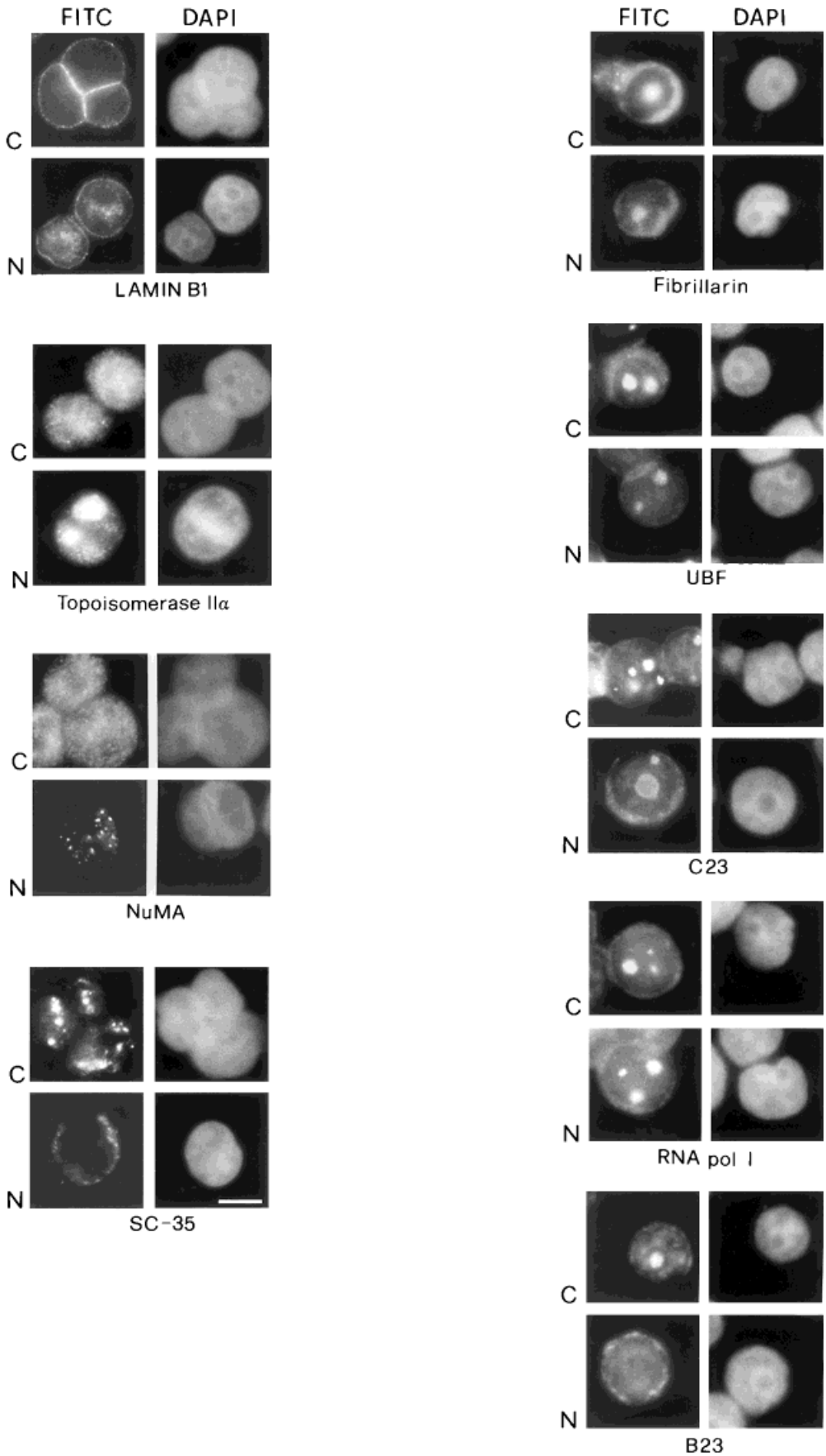

Fig. 2. Immunofluorescence staining of control (C) and necrotic (N) HL-60 cells. Scale bar: 5 μm.

TABLE I. Percent of Necrotic Cells Showing Typical Changes (as described in the text) in the Spatial Distribution Pattern of Nuclear Polypeptides

Protein	Percent of cells showing changes in the immunofluorescence pattern
Lamin B1	71.6±8.3
Topoisomerase IIα	79.5±9.9
NuMA	68.7±8.8
SC-35	74.5±10.4
B23	89.1±9.5

nant cleavage product of approximately 110 kDa. Only traces of this fragment were seen in necrotic cells (Fig. 4). In etoposide-treated cells, two major cleavage products of NuMA protein were detected, banding at approximately 200- and 185 kDa. In contrast, in necrotic samples NuMA was proteolytically degraded to multiple smaller fragments, in the range of 105/130 kDa (Fig. 4). Apoptotic cleavage of NuMA was completely blocked by an inhibitor of caspase-6 (VEID-CHO) but not by Ac-DEVD-CMK, which inhibits caspase-3. On the other hand, VEID-CHO could not prevent the necrotic proteolysis of NuMA. Also Ac-DEVD-CMK, Z-IETD-FMK (an inhibitor of caspase-8), and Z-LEHD-FMK (an inhibitor of caspase-9) were completely ineffective in this sense (data not presented). Consistent with other reports [Goehring et al., 1997; Kipp et al., 2000], SAF-A was cleaved during apoptosis into the signature 97 kDa fragment. This fragment was absent from lysates of necrotic cells, in which instead we detected a cleavage product banding at approximately 102 kDa (Fig. 4). Ac-DEVD-CMK reduced the amount of the 97 kDa fragment seen in extracts from apoptotic cells, whereas VEID-CHO could not. All the caspase inhibitors we tested did not block the necrotic cleavage of SAF-A (Fig. 4 and data not presented). The signature 70 kDa fragment of SATB1 was detected in both apoptotic and necrotic samples. However, in ethanol-treated HL-60 cells, in addition to the signature fragment, we observed a larger fragment with a Mr of about 84 kDa (Fig. 4). Apoptotic proteolysis of SATB1 was markedly inhibited by VEID-CHO but not by Ac-DEVD-CMK. In contrast, VEID-CHO could not prevent the proteolytic cleavage of SATB1 in necrotic samples (Fig. 4). Ac-DEVD-CMK, Z-IETD-FMK, and Z-LEHD-FMK were also ineffective in this sense (data not shown).

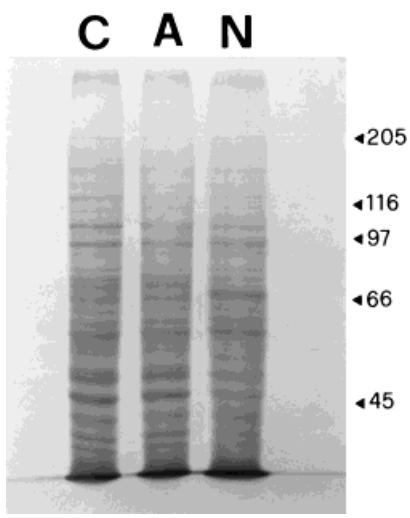

Fig. 3. SDS-PAGE of proteins from whole cell extracts. 80 μg of protein was separated on a 10% gel. The position of molecular weight markers is indicated. C: control cells; A: apoptotic cells; N: necrotic cells.

The splicing component SC-35 did not show any sign of cleavage during either apoptosis or necrosis (Fig. 4). However, in samples from apoptotic cells we observed a slight reduction in the intensity of the immunoreactivity. Thus, it might be that some proteolysis had indeed occurred, but the monoclonal antibody we used could not recognize the cleaved fragment(s). The nucleolar protein C23/nucleolin was largely uncleaved during apoptosis, even though we detected an extremely faint band of 97 kDa after a 5 h treatment with etoposide. No cleavage at all was detectable in necrotic HL-60 cells. Protein B23 was also uncleaved both in apoptotic and necrotic HL-60 cells (Fig. 4). This is in agreement with Casiano et al. [1998]. A down-regulation of B23/nucleophosmin had been demonstrated to occur in apoptotic Jurkat T lymphoblasts [Patterson et al., 1995].

In Table II we summarize the results of both the immunofluorescence staining and the immunoblotting analysis.

TEM Analysis of HL-60 Cell Nuclear Matrix

As shown in Figure 5A, the nuclear matrix prepared from untreated HL-60 cells exhibited a characteristic tripartite structure, with an outer lamina, an inner fibrogranular network, and nucleolar remnants. The tripartite organization was somewhat maintained also in necrotic nuclear matrices, albeit the inner fibrogranular network was more rarified (Fig. 5B).

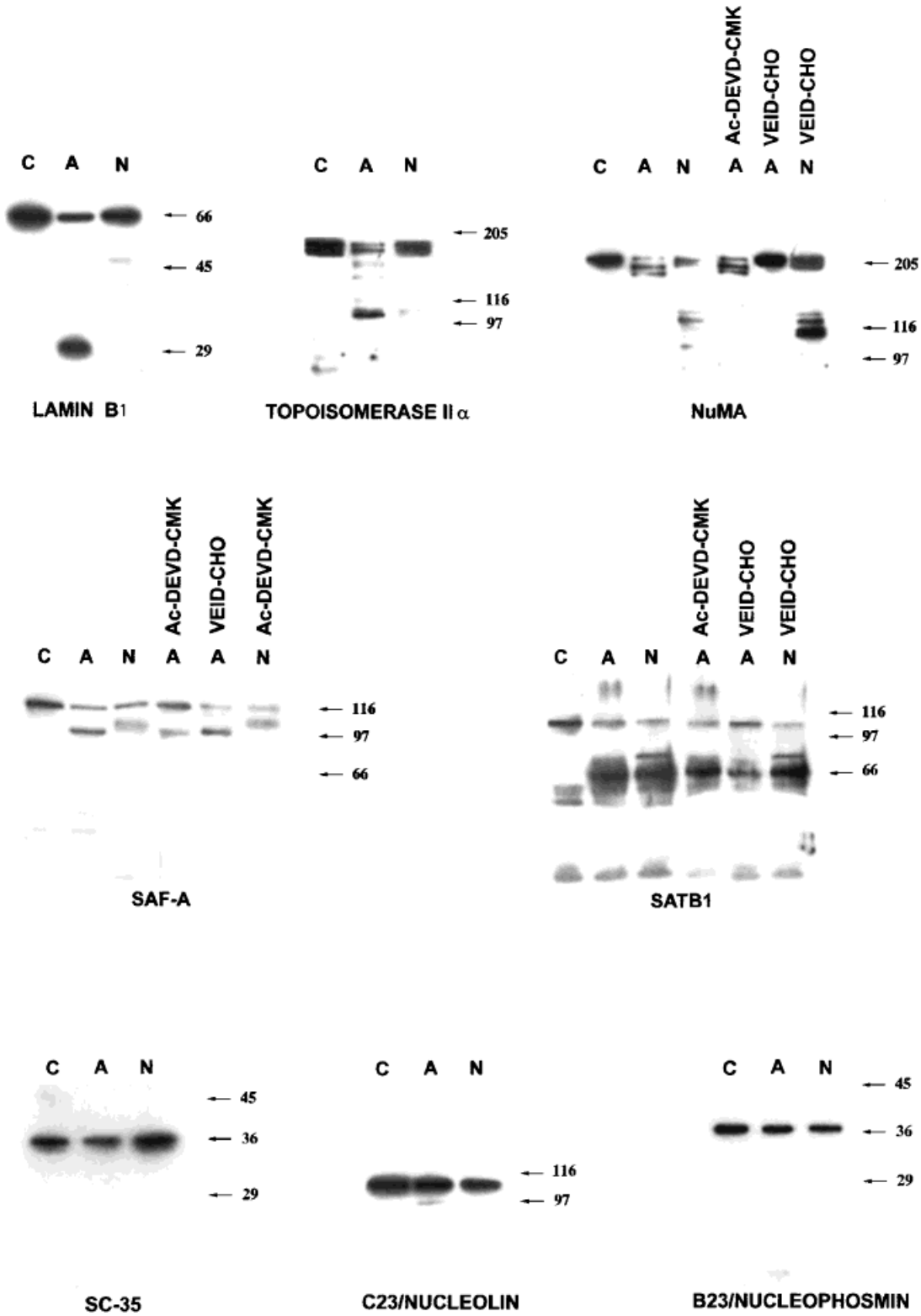

Fig. 4. Immunoblots showing cleavage of some nuclear proteins during apoptosis or necrosis. The position of molecular weight markers is indicated. C: control cells; A: apoptotic cells; N: necrotic cells. Cells (1×10^7) were lysed in 1 ml of electrophoresis sample buffer, briefly sonicated, and boiled. Protein was separated by SDS-PAGE and transferred to nitrocellulose sheets that were then probed with monoclonal or polyclonal antibodies to various nuclear polypeptides. Bands were visualized by the enhanced chemiluminescence method.

TABLE 2. Summary of the Results Obtained by Immunofluorescence Staining and Immunoblotting Analysis

Protein	Immunofluorescence changes in necrotic cells	Proteolysis in apoptotic cells and size of predominant fragments(s)	Proteolysis in necrotic cells and size of predominant fragments(s)
Lamin B1	Yes	Yes:28 kDa	Very slight: 50 kDa
Topoisomerase IIα	Yes	Yes:110 kDa	Very slight: 110 kDa
NuMA	Yes	Yes:200-and 185 kDa	Yes: multiple at 130 /105 kDa
SC-35	Yes	No	No
SAF-A	n.p.	Yes:97 kDa	Yes:102 kDa
SATB1	n.p.	Yes:70 kDa	Yes:84-and 70 kDa
Fibrillarin	No	n.p.	n.p.
UBF	No	n.p.	n.p.
C23	No	Very slight: 97 kDa	No
RNA polymerase I	No	n.p.	n.p.
B23	Yes	No	No

n.p., not performed

The interchromatin granules were not clustered, as observed in control matrices, but instead they were homogeneously distributed. The nucleolar remnants of necrotic matrices were sharply separated from the fibrogranular network. Furthermore, ultrastructural analysis revealed that preparations of necrotic nuclear matrices were always contaminated by residual elements of the cytoskeleton (see also later). We could never avoid such a contamination, even if we employed a higher (up to 1%) concentration of detergent (Triton X-100 or Nonidet P-40) in the TM-2 buffer during the preparation of nuclei (data not presented).

Protein Composition of Necrotic Nuclear Matrix

We next investigated the protein composition of necrotic HL-60 cell nuclear matrix by means of two-dimensional gel electrophoresis. As presented in Figure 6, it was possible to appreciate both quantitative and qualitative differences between normal and necrotic samples (compare A with B). As a whole, the necrotic nuclear matrix fraction retained more protein (about 50%) than that prepared from normal cells. However, it is likely that most of the differences we detected were due to contamination problems. To prove that the matrix from ethanol-treated cells was contaminated by components of the cytoskeleton, we performed immunoblotting with an antibody to β-tubulin. As shown in Figure 6 (panel C) β-tubulin was absent from preparations of control nuclear matrix (lane 1). However, when the nuclear matrix was obtained from necrotic cells a strong reaction for β-tubulin (Mr 55 kDa) was observed (lane 2).

DISCUSSION

In this paper, we have reported the results of an investigation designed to analyze the changes that possibly occur in the nucleus during necrosis and to compare them to the modifications taking place in the same organelle during apoptosis. As far as changes in the localization of nuclear components are concerned, those regarding topoisomerase IIα are of particular interest, because we never observed similar modifications in apoptotic cells, where the immunoreactivity for topoisomerase IIα was markedly lower than in control cells (R. Bortul, unpublished experiments). Given also that the changes in the spatial distribution of topoisomerase IIα have been detected with other necrosis-inducing agents ($HgCl_2$, H_2O_2, heat) and in other cell lines (Jurkat T lymphoblasts) (R. Bortul, unpublished experiments), we think that immunostaining with an antibody to topoisomerase IIα might be a useful way to distinguish between apoptotic and necrotic cells.

The changes in the spatial distribution of other nuclear proteins during necrosis were not as striking or were similar to those occurring during apoptosis. We think that the modifications we have seen in the lamin B1 fluorescence pattern are conceivably due to changes in the overall organization of the necrotic nucleus that unmask intranuclear lamin B1 and render it accessible to the antibody.

When the possible cleavage patterns of eight nuclear components were examined employing whole cell extracts from necrotic and apoptotic samples, our results were essentially similar to

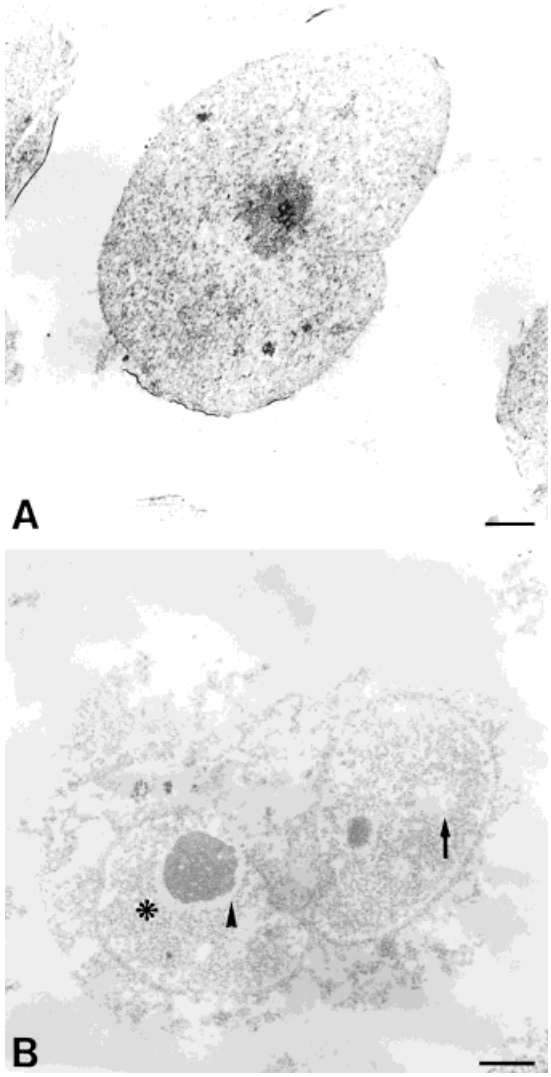

Fig. 5. TEM analysis of control and necrotic HL-60 cell nuclear matrix. **(A):** control nuclear matrix. **(B):** nuclear matrix obtained from ethanol-exposed cells; the asterisk points to the fibrogranular network; arrow indicates a transparent area; arrowhead points to a nucleolar remnant sharply separated from the fibrogranular network. Scale bar: 1 μm.

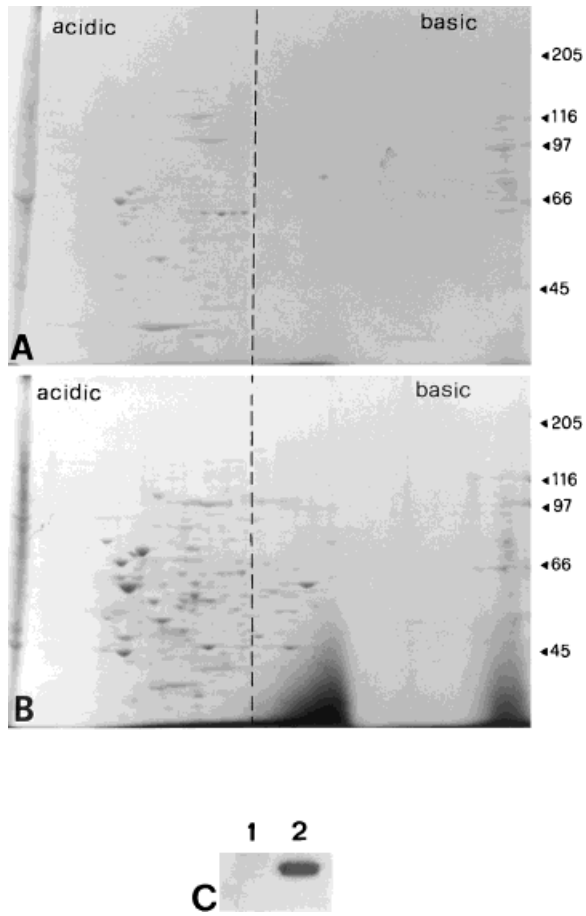

Fig. 6. Two-dimensional gel electrophoresis analysis of protein recovered in the nuclear matrix prepared from control (**panel A**) and ethanol-treated (**panel B**) HL-60 cells. Migration in the first dimension (NEPHGE) was from left to right. The dashed line indicates pH 7.0. Molecular weight markers are indicated on the left. Panel C: immunoblot showing the presence of μ-tubulin in the nuclear matrix prepared from necrotic cells (lane 2). Lane 1: nuclear matrix obtained from control cells. 50 μg of protein was blotted to each lane. The observed Mr was 55 kDa.

those reported by Casiano et al. [1998] who demonstrated that during necrosis several nuclear proteins are either not cleaved or cleaved in a pattern which differs from that peculiar to apoptosis.

The only notable exception we have observed is represented by SATB1, because the apoptotic signature cleavage fragment of 70 kDa was also generated in necrotic cells in an amount similar to apoptotic cells.

We would like to point out that in an our previous report we did not detect apoptotic cleavage of SATB1 protein after treatment with camptothecin [Martelli et al., 1999a]. However, in the present study, in which we employed etoposide, we observed the characteristic apoptotic signature cleavage pattern of SATB1, as reported recently also by others [Gotzmann et al., 2000]. A possible explanation is that different apoptotic effectors cause the generation of different cleavage patterns, in agreement with the recent findings by Dynlacht et al. [2000].

As far as the results of the inhibition of caspases are concerned, our data are in line with the data reported by others [Casiano et al., 1998] who showed that the proteolytic cleavage which takes place during necrosis is not blocked by the commonly employed caspase inhibitors.

Thus, other proteases, that await precise identification, must be activated during necrosis. However, at least in the case of SATB1, the caspase inhibitor-insensitive proteolytic activity was capable of generating the apoptotic signature fragment of 70 kDa in necrotic cells.

The fact that apoptotic cleavage of SAF-A was inhibited by Ac-DEVD-CMK is consistent with this protein being a target of caspase-3 [Kipp et al., 2000]. At variance with Gotzmann et al. [2000], the cleavage of SATB1 in apoptotic samples was not prevented by treatment of cells with an inhibitor of caspase-3, but it was indeed largely reduced by VEID-CHO, which inhibits caspase-6. However, Gotzmann et al. [2000] have mapped a potential caspase-6 cleavage site (VEMD) in the N-terminal site of SATB1. Thus, it would seem more logical that an inhibitor of caspase-6 could prevent proteolysis.

In necrotic cells, three nuclear proteins which are thought to play an important structural role (i.e. NuMa, SAF-A, and SATB1) were cleaved. Indeed, these proteins (as well as topoisomerase IIα) bind to specific DNA sequences, called Scaffold or Matrix Associated Regions (S/MARs) that would represent 300–1000 bp long stretches of nucleotides, A-T rich (over 70%), conceivably defining the base of loops in which genomic DNA is organized during the interphase. As strong evidence has been presented that S/MARs are essential determinants of chromatin structure, the proteins binding to these elements can be considered putative structural components of the nuclear matrix [Strick and Laemmli, 1995].

It may, therefore, appear somewhat surprising that we did not detect dramatic changes in the nuclear matrix structure of ethanol-treated cells. This could not be the consequence of the stabilization with NaTT, because our own previous results have demonstrated that, if the cells are apoptotic, morphological modifications of the nuclear matrix were evident even though nuclei had been exposed to NaTT prior to DNase I digestion and 2 M NaCl extraction [Martelli et al., 1999b]. A few points should be taken into account for a possible explanation. As far as NuMA is concerned, previous investigations, in which a mutated form of NuMA was overexpressed, have suggested that it could play a major structural role in the architecture of the normal interphase nucleus [Gueth-Hallonet et al., 1998], even if more recent results have questioned such a conclusion [Taimen et al., 2000], because NuMA can be lost by non-proliferating cells without dramatic effects on nuclear structure and shape. Moreover, the cleavage pattern of both NuMA and SAF-A in necrotic cells differs from that observed in apoptotic samples, as emphasized above. These differences might affect in a specific manner the overall organization of the nuclear matrix so that it did not degrade as much as during apoptosis. Furthermore, in necrotic samples an important structural protein such as topoisomerase IIα [e.g. Adachi et al., 1989] was almost completely uncleaved. However, it might be that in this respect the most critical issue is the absence of lamin B1 proteolysis in necrotic cells. Evidence indicates that lamin cleavage is very important for the occurrence of the nuclear changes typical of apoptosis. Indeed, Rao and coworkers [1996] have shown that overexpression of uncleavable mutant lamin A or B blocks the appearance of chromatin condensation and nuclear shrinkage typical of apoptotic cell death, even though the late stages of apoptosis were morphologically unaltered and formation of apoptotic bodies was evident. Lazebnik et al. [1995] had previously reported that lamin proteolysis is a prerequisite also for chromatin packaging into apoptotic bodies.

Finally, the possibility exists that the ethanol treatment we employed to induce necrosis acted as a mild fixative also for the nuclear matrix (and not only for the cytoskeletal elements) and this fact would have prevented marked changes in the nuclear matrix.

In any case, our results, taken together, unequivocally show that marked nuclear changes occur also during necrotic cells death. The changes are partly similar and partly different form those taking place during apoptosis. The nuclear matrix is affected by this type of death (even though only partially) and this is somewhat consistent with the report by Dynlacht et al. [1999]. It might be hypothesized that both the rarefaction of matrix inner fibrogranular network and the homogeneous distribution of interchromatin granules seen during necrosis are the consequence of the specific cleavage of SAF-A and NuMA. Indeed, both of these proteins associate with nuclear ribonucleoprotein complexes [Zeng et al., 1994; Kipp et al., 2000], that are among the most abundant components of the nuclear matrix [Berezney, 1991; Berezney et al., 1995]. A different proteolytic cleavage of SAF-A and NuMA, associated

with cleavage of SATB1 and lamin B1, may lead to the more striking changes that are typical of the nuclear matrix prepared from apoptotic cells [Martelli et al., 1999a, 1999b].

It may be that the differential immunostaining and proteolytic cleavage patterns we have identified prove to be useful in the future for allowing a differential diagnosis between necrotic and apoptotic samples, especially in the context of pathological processes in vivo, which has never been an easy task if ultrastructural analysis could not be employed [Farber, 1994; Columbano, 1995; Majno and Joris, 1995].

ACKNOWLEDGMENT

We thank Giovanna Baldini for helpful technical assistance.

REFERENCES

Adachi Y, Kas E, Laemmli UK. 1989. Preferential, cooperative binding of DNA topoisomerase II to scaffold-associated regions. EMBO J 13:3997–4006.

Bellamy OC, Malcomson DG, Harrison DJ, Wyllie AH. 1995. Cell death in health and disease: the biology and regulation of apoptosis. Semin Cancer Biol 6:3–16.

Berezney R. 1991. The nuclear matrix: a heuristic model for investigating genomic organization and function in the cell nucleus. J Cell Biochem 47:109–123.

Berezney R, Mortillaro M J, Ma H, Wei X, Samarabandu J. 1995. The nuclear matrix: a structural milieu for genomic function. Int Rev Cytol 162A:1–65.

Biggiogera M, Trenatani A, Martin TE, Pellicciari C. 1999. Terminal differentiation of erythroblasts leads to RNP segregation and formation of heterogeneous ectopic RNP-derived structures. Histochem Cell Biol 112: 473–477.

Bradford MM. 1976. A rapid and sensitive method for the quantitation of microgram quantities of protein utilizing the principle of protein dye binding. Anal Biochem 72: 248–254.

Buendia B, Santa-Maria A, Courvalin JC. 1999. Caspase-dependent proteolysis of integral and peripheral proteins of nuclear membranes and nuclear pore complex proteins during apoptosis. J Cell Sci 112:1743–1753.

Casiano CA, Martin SJ, Green DR, Tang EM. 1996. Selective cleavage of nuclear autoantigens during CD95(Fas/APO-1)-mediated T cell apoptosis. J Exp Med 184:765–770.

Casiano CA, Ochs RL, Tan EM. 1998. Distinct cleavage products of nuclear proteins in apoptosis and necrosis revealed by autoantibody probes. Cell Death Diff 5:183–190.

Columbano A. 1995. Cell death: current difficulties in discriminating apoptosis from necrosis in the context of pathological processes in vivo. J Cell Biochem 58:181–190.

Degen WGJ, Pruijn GJM, Raats JM, van Venrooij WJ. 2000. Caspase-dependent cleavage of nucleic acids. Cell Death Diff 7:616–627.

Duband-Goulet I, Courvalin JC, Buendia B. 1998. LBR, a chromatin and lamin binding protein from the inner nuclear membrane, is proteolyzed at late stages of apoptosis. J Cell Sci 111:1441–1451.

Dynlacht JR, Earles M, Henthorn J, Roberts ZV, Howard EW, Seno JD, Sparling D, Story MD. 1999. Degradation of the nuclear matrix is a common element during radiation-induced apoptosis and necrosis. Radiat Res 152:590–603.

Dynlacht JR, Earles M, Henthorn J, Seno JD. 2000. Different patterns of DNA fragmentation and degradation of nuclear matrix proteins during apoptosis induced by radiation, hyperthermia or etoposide. Radiat Res 152:590–603.

Earnshaw WC. 1995. Nuclear changes in apoptosis. Curr Opin Cell Biol 7:337–343.

Farber E. 1994. Programmed cell death: necrosis vs. apoptosis. Modern Pathol 7:605–609.

Faraco PR, Ledgerwood EC, Vandenabeele P, Prons JB, Bradley JR. 1999. Tumour necrosis factor induces distinct patterns of caspase activation in WEHI-164 cells associated with apoptosis or necrosis depending on cell cycle stage. Biochem Biophys Res Comm 261:385–392.

Gerner C, Seelos C, Sauermann G. 1998. Alteration of nuclear matrix protein composition during apoptosis in rat embryo cells. Exp Cell Res 238:472–480.

Goehring F, Schwab BL, Nicotera P, Leist M, Fackelmayer FO. 1997. The novel SAR-binding domain of scaffold attachment factor A (SAF-A) is a target in apoptotic nuclear breakdown. EMBO J 16:7361–7371.

Gotzmann J, Meissner M, Gerner C. 2000. The fate of the nuclear matrix-associated-region-binding protein SATB1 during apoptosis. Cell Death Diff 7:425–438.

Gueth-Hallonet C, Wang J, Harborth J, Weber K, Osborn M. 1998. Induction of a regular lattice by overexpression of NuMA. Exp Cell Res 243:434–452.

Kipp M, Schwab BL, Przybylski M, Nicotera P, Fackelmayer FO. 2000. Apoptotic cleavage of scaffold attachment factor A (SAF-A) by caspase-3 occurs at a noncanonical cleavage site. J Biol Chem 275:5031–5036.

Lazebnik YA, Takahashi A, Moir RD, Goldman RD, Poirier GG, Kaufmann SH, Earnshaw WC. 1995. Studies of the lamin proteinase reveal multiple parallel biohemical pathways during apoptotic execution. Proc Natl Acad Sci USA92:9042–9046.

Majno G, Joris I. 1995. Apoptosis oncosis and necrosis: an overview of cell death. Am J Pathol 146:3–15.

Martelli AM, Cocco L, Riederer BM, Neri LM. 1996. The nuclear matrix: a critical appraisal. Histol Histopathol 11:1035–1048.

Martelli AM, Bareggi R, Bortul R, Grill V, Narducci P, Zweyer M. 1997. The nuclear matrix and apoptosis. Histochem Cell Biol 108:1–10.

Martelli AM, Bortul R, Fackelmayer FO, Tazzari PL, Bareggi R, Narducci P, Zweyer M. 1999a. Biochemical and morphological characterization of the nuclear matrix from apoptotic HL-60 cells. J Cell Biochem 72:35–46.

Martelli AM, Bortul R, Bareggi R, Grill V, Narducci P, Zweyer M. 1999b. Biochemical and morphological changes in the nuclear matrix prepared from apoptotic HL-60 cells. Effect of different stabilizing procedures. J Cell Biochem 74:99–110.

Martelli AM, Robuffo I, Bortul R, Ochs RL, Luchetti F, Cocco L, Zweyer M, Bareggi R, Falcieri E. 2000. Behavior

of nucleolar proteins during the course of apoptosis in camptothecin-treated HL-60 cells. J Cell Biochem 78: 264–277.

O'Farrell PH. 1975. High-resolution two-dimensional electrophoresis of proteins. J Biol Chem 250:4007–4021.

O'Farrell PZ, Goodman HM, O'Farrell PH. 1977. High-resolution two-dimensional electrophoresis of basic as well acidic proteins. Cell 12:1133–1142.

Patel T, Gores GJ, Kaufmann SH. 1996. The role of proteases during apoptosis. FASEB J 10:587–597.

Patterson SD, Grossman JS, D'Andrea P, Latter GI. 1995. Reduced numatrin/B23/nucleophosmin in apoptotic Jurkat T-lymphoblasts. J Biol Chem 270:9429–9436.

Rao L, Perez D, White E. 1996. Lamin proteolysis facilitates nuclear events during apoptosis. J Cell Biol 135:1441–1455.

Shah GM, Shah RG, Poirier GG. 1996. Different cleavage patterns for poly(ADP-ribose) polymerase during necrosis and apoptosis in HL-60 cells. Biochem Biophys Res Comm 229:838–844.

Shimizu S, Eguchi Y, Kamiike W, Waguri S, Uchiyama Y, Matsuda H, Tsujimoto Y. 1996. Retardation of chemical hypoxia-induced necrotic cell death by BCL-2 and ICE inhibitors: possible involvement of common mediators in apoptotic and necrotic signal transductions. Oncogene 12:2045–2050.

Strick R, Laemmli UK. 1995. SARs are cis DNA elements of chromosome dynamics: synthesis of a SAR repressor protein. Cell 83:1137–1148.

Taimen P, Viljamaa M, Kallajoki M. 2000. Preferential expression of NuMA in the nuclei of proliferating cells. Exp Cell Res 256:140–149.

Thornberry NA, Lazebnik Y. 1998. Caspases: enemies within. Science 281:1312–1316.

Utz PJ, Anderson P. 2000. Life and death decisions: regulation of apoptosis by proteolysis of signaling molecules. Cell Death Diff 7:589–602.

Waterhouse N, Kumarz S, Song Q, Strike P, Sparrow L, Dreyfuss G, Alnemri ES, Litwack G, Lavin M, Watters D. 1996. Heteronuclar ribonucleoproteins C1 and C2, components of the spliceosome, are specific targets of interleukin 1β-converting enzyme-like proteases in apoptosis. J Biol Chem 271:29335–29341.

Weaver VM, Carson CE, Walker PR, Chaly N, Lach B, Raymond Y, Brown DL, Sikorska M. 1996. Degradation of nuclear matrix and DNA cleavage in apoptotic thymocytes. J Cell Sci 109:45–56.

Wyllie AH, Kerr JFR, Currie AR. 1980. Cell death: the significance of apoptosis. Int Rev Cytol 68:251–306.

Zeng C, He D, Berget SM, Brinkley BR. 1994. Nuclear-mitotic apparatus protein: a structural protein between the nucleoskeleton and RNA splicing. Proc Natl Acad Sci USA91:1505–1509.

Zweyer M, Bareggi R, Grill V, Soranzo MR, Marugg RA, Riederer BM, Narducci P, Martelli AM. 1995. Behaviour of nuclear matrix proteins during camptothecin-induced apoptosis in HL-60 human leukemia cells. Exp Cell Res 221:27–40.

Zweyer M, Riederer BM, Ochs RL, Fackelmayer FO, Kohwi-Shigematsu T, Bareggi R, Narducci P, Martelli AM. 1997. Association of nuclear matrix proteins with fibrogranular nuclear bodies in cell lines undergoing apoptosis. Exp Cell Res 230:325–336.